reactor. After the appropriate time, the solvent was evaporated under a stream of nitrogen and the residual material dissolved in $CDCl_3$. NMR spectra were recorded with a Varian 400-MHz spectrometer.

The laser flash photolysis apparatus has been described.[8]

Facile Transformations of 12- and 13-Vertex Tungstacarborane Polyhedra: Reversible Framework Rearrangement and Acid-Induced Ejection of a Cage Vertex[1]

Stephen A. Brew,[2a] Nicholas Carr,[2b] John C. Jeffery,[2a] Massimino U. Pilotti,[2a] and F. Gordon A. Stone*,[2b]
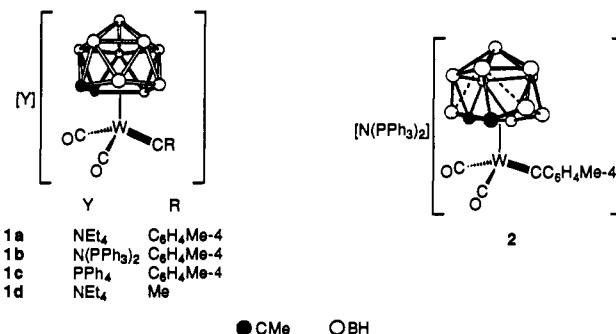
Contribution from the Department of Inorganic Chemistry, The University, Bristol BS8 1TS, U.K., and Department of Chemistry, Baylor University, Waco, Texas 76798-7348. Received August 6, 1991

Abstract: Reactions of [Y][*closo*-1,2-Me_2-3-($\equiv$CR)-3,3-$(CO)_2$-3,1,2-$WC_2B_9H_9$] (Y = NEt_4, $N(PPh_3)_2$, PPh_4; R = Me, C_6H_4Me-4) with aqueous HX (X = Cl, I) afforded the salts [Y][*closo*-1,8-Me_2-11-(CH_2R)-2-X-2,2,2-$(CO)_3$-2,1,8-$WC_2B_9H_8$]; the structure of the product with X = Cl, Y = NEt_4, and R = C_6H_4Me-4 has been established by X-ray diffraction. A notable structural feature of the anion is that the carborane CMe groups do not occupy adjacent vertices, unlike the situation in the alkylidyne precursor complex. This observation is particularly remarkable in that the framework rearrangement occurs rapidly at temperatures as low as −78 °C. In addition, one of the boron atoms in the lower pentagonal ring of the cage carries a $CH_2C_6H_4$Me-4 substituent which evidently results from insertion of an initially formed alkylidene fragment into a cage B–H bond. Reactions between the salts [Y][*closo*-1,8-Me_2-11-(CH_2R)-2-X-2,2,2-$(CO)_3$-2,1,8-$WC_2B_9H_8$] and 1 mol equiv of $AgBF_4$ in the presence of CO gave the compounds [*closo*-1,8-Me_2-11-(CH_2R)-2,2,2,2-$(CO)_4$-2,1,8-$WC_2B_9H_8$] in which the cage CMe groups remain separated. In contrast, an excess of the reagent $AgBF_4$ afforded a 1:1 mixture of the same species and the compounds [*closo*-1,2-Me_2-8-(CH_2R)-3,3,3,3-$(CO)_4$-3,1,2-$WC_2B_9H_8$] containing adjacent CMe groups. These reactions are reversible: Addition of NEt_4Cl to tetrahydrofuran solutions of the tetracarbonyl species regenerates [NEt_4][*closo*-1,8-Me_2-11-(CH_2R)-2-Cl-2,2,2-$(CO)_3$-2,1,8-$WC_2B_9H_8$]. This is a very rare example of a reversible polytopal rearrangement of CMe groups. Reactions between [Y][*closo*-1,8-Me_2-11-$(CH_2C_6H_4$Me-4)-2-X-2,2,2-$(CO)_3$-2,1,8-$WC_2B_9H_8$] and the alkynes PhC$\equiv$CR' (R' = Ph, Me) in the presence of $AgBF_4$ readily afforded the (alkyne)tungstacarborane complexes [*closo*-1,8-Me_2-11-$(CH_2C_6H_4$Me-4)-2,2-$(CO)_2$-2-(η-PhC_2R')-2,1,8-$WC_2B_9H_8$]. An X-ray diffraction study of one of these (R' = Me) confirmed the structure. Protonation of the salt [$N(PPh_3)_2$][*closo*-1,6-Me_2-4-($\equiv$CC_6H_4$Me-4)-4,4-$(CO)_2$-4,1,6-$WC_2B_{10}H_{10}$] with HX (X = Cl, I) yielded the salts [$N(PPh_3)_2$][*closo*-1,7-Me_2-2-X-2,2,2-$(CO)_3$-2,1,7-$WC_2B_9H_9$], for which an X-ray diffraction study (X = I) revealed that a 13- to 12-vertex cage degradation had occurred, as well as loss of a CC_6H_4Me-4 fragment. This degradation is remarkable considering the acidic reaction conditions. In addition to the three X-ray diffraction studies, the new compounds were characterized by microanalysis; ^1H, ^{13}C, and ^{11}B NMR spectroscopy; and infrared spectroscopy.

Introduction

We have recently been exploring the chemistry of salts of the anionic alkylidynecarborane complexes [*closo*-1,2-Me_2-3-($\equiv$CR)-3,3-$(CO)_2$-3,1,2-$MC_2B_9H_9$]⁻ (**1**; M = Mo, W; R = alkyl, alkynyl, aryl) and [*closo*-1,6-Me_2-4-($\equiv$CC_6H_4$Me-4)-4,4-$(CO)_2$-4,1,6-$MC_2B_{10}H_{10}$]⁻ (**2**; M = Mo, W).[3] Our initial studies concentrated on the use of these complexes for the synthesis of compounds containing metal–metal bonds, and numerous di-, tri-, and polynuclear metal species have now been prepared.[4] During this early work, the carborane cage was used as an isolobal replacement for the more widely studied cyclopentadienyl ligand. Thus, the metal atom was regarded as η^5 coordinated by the open pentagonal CCBBB face of a nido 11-vertex dianion [7,8-$C_2B_9H_9Me_2$]²⁻ or η^6 coordinated by the puckered CBCBBB face of a nido 12-vertex dianion [7,9-$C_2B_{10}H_{10}Me_2$]²⁻. Although the first results supported the use of this formalism, in many of these reactions the carborane ligand does not adopt a spectator role,

leading to the frequent observation of exopolyhedral B–H → M or B–M (metal) bonds, or insertion of the alkylidyne ligand into a B–H bond of the cage to give a BCH_2R fragment. Consequently, we have preferred to regard anions of the salts **1** and **2**, respec-

1a	NEt_4	C_6H_4Me-4
1b	$N(PPh_3)_2$	C_6H_4Me-4
1c	PPh_4	C_6H_4Me-4
1d	NEt_4	Me

● CMe   ○ BH

tively, as 12-vertex icosahedral and 13-vertex docosahedral *closo*-metallacarboranes, with the added spice of a reactive and indeed interactive alkylidyne ligand on the periphery of the cage.

Lately we have focused upon protonation reactions of these salts. This work was prompted by our earlier observation[5] that treatment

(1) (a) Alkylidyne(carbaborane) Complexes of the Group 6 Metals. 3. (b) Part 2: Brew, S. A.; Jenkins, P. D.; Jeffery, J. C.; Stone, F. G. A. *J. Chem. Soc., Dalton Trans.* **1992,** 401.

(2) (a) The University, Bristol. (b) Baylor University.

(3) (a) Brew, S. A.; Carr, N.; Mortimer, M. D.; Stone, F. G. A. *J. Chem. Soc., Dalton Trans.* **1991,** 811. Cabioch, J.-L.; Dossett, S. J.; Hart, I. J.; Pilotti, M. U.; Stone, F. G. A. *J. Chem. Soc., Dalton Trans.* **1991,** 519. Carr, N.; Fernandez, J. R.; Stone, F. G. A. *Organometallics* **1991,** *10,* 2718.

(4) Stone, F. G. A. *Adv. Organomet. Chem.* **1990,** *31,* 53.

(5) Howard, J. A. K.; Jeffery, J. C.; Laurie, J. C. V.; Moore, I.; Stone, F. G. A.; Stringer, A. *Inorg. Chim. Acta* **1985,** *100,* 23.

Table I. Physical and Infrared Absorption Data[a]

compound	color	yield (%)	$\nu_{max}(CO)^b/cm^{-1}$
[NEt$_4$][*closo*-1,8-Me$_2$-11-(CH$_2$C$_6$H$_4$Me-4)-2-Cl-2,2,2-(CO)$_3$-2,1,8-WC$_2$B$_9$H$_8$] (9a)	yellow	46	2013 s, 1916 s (br)
[N(PPh$_3$)$_2$][*closo*-1,8-Me$_2$-11-(CH$_2$C$_6$H$_4$Me-4)-2-I-2,2,2-(CO)$_3$-2,1,8-WC$_2$B$_9$H$_8$] (9b)	orange	50	2007 s, 1917 s (br)
[NEt$_4$][*closo*-1,8-Me$_2$-11-Et-2-I-2,2,2-(CO)$_3$-2,1,8-WC$_2$B$_9$H$_8$] (9d)	ochre	40	2007 s, 1916 s (br)
[*closo*-1,8-Me$_2$-11-(CH$_2$C$_6$H$_4$Me-4)-2,2,2,2-(CO)$_4$-2,1,8-WC$_2$B$_9$H$_8$] (10a)	yellow	95	2091 s, 2023 m, 2011 m (sh), 1974 s
[*closo*-1,8-Me$_2$-11-Et-2,2,2,2-(CO)$_4$-2,1,8-WC$_2$B$_9$H$_8$] (10b)	yellow	92	2089 s, 2019 s, 2007 m (sh), 1976 vs^c
[*closo*-1,8-Me$_2$-11-(CH$_2$C$_6$H$_4$Me-4)-2-(η-PhC$_2$Ph)-2,2-(CO)$_2$-2,1,8-WC$_2$B$_9$H$_8$] (11a)	purple	80	2043 s, 1982 s
[*closo*-1,8-Me$_2$-11-(CH$_2$C$_6$H$_4$Me-4)-2-(η-MeC$_2$Ph)-2,2-(CO)$_2$-2,1,8-WC$_2$B$_9$H$_8$] (11b)	purple	93	2040 s, 1976 s
[N(PPh$_3$)$_2$][*closo*-1,7-Me$_2$-2-Cl-2,2,2-(CO)$_3$-2,1,7-WC$_2$B$_9$H$_9$] (12a)	orange	46	2023 s, 1933 m (sh), 1916 s
[N(PPh$_3$)$_2$][*closo*-1,7-Me$_2$-2-I-2,2,2-(CO)$_3$-2,1,7-WC$_2$B$_9$H$_9$] (12b)	orange	47	2013 s, 1930 m (sh), 1910 s

[a] Satisfactory analytical data (C, H, N) have been obtained for all new compounds. [b] Measured in CH$_2$Cl$_2$ unless otherwise stated. All complexes show a weak, very broad absorption at ~2550 cm^{-1} due to BH stretching. Legend: vs, very strong; s, strong; m, medium; sh, shoulder; br, broad. [c] Measured in Et$_2$O.

of the isolobal cyclopentadienyl analogue [W($\equiv$CR)(CO)$_2$(η-C$_5$H$_5$)] (R = C$_6$H$_4$Me-4) with HBF$_4$·Et$_2$O gave the (μ-alkyne)-ditungsten salt [W$_2$(μ-H)(μ-RC$_2$R)(CO)$_4$(η-C$_5$H$_5$)$_2$][BF$_4$] (3), evidently via the intermediacy of a cationic alkylidene species [W{=C(H)R}(CO)$_2$(η-C$_5$H$_5$)]$^+$. With HI as the protonating agent the stable alkylidene complex [W{=C(H)R}I(CO)$_2$(η-C$_5$H$_5$)] was isolated, thereby capturing the intermediate species suggested by the HBF$_4$·Et$_2$O studies.
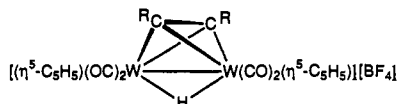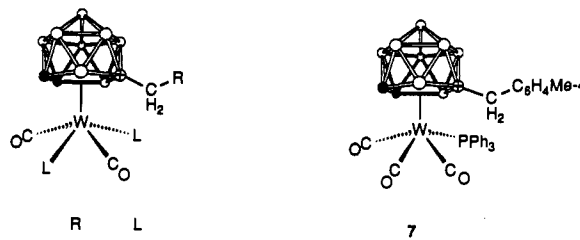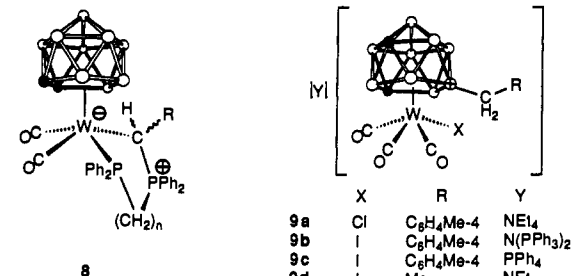

3   R = C$_6$H$_4$Me-4

We suspected that the presence of the polyhedral WC$_2$B$_9$ or WC$_2$B$_{10}$ fragments in the salts 1 and 2 would influence the nature of the products obtained from protonation of the M$\equiv$C bonds, since migration and insertion reactions are possibilities that are not readily available to their cyclopentadienyl analogues. In the preceding papers of this series[1b,6] we have described the results obtained by protonating the salts [Y][*closo*-1,2-Me$_2$-3-($\equiv$CR)-3,3-(CO)$_2$-3,1,2-WC$_2$B$_9$H$_9$] (Y = NEt$_4$, R = C$_6$H$_4$Me-4, 1a; Y = PPh$_4$, R = C$_6$H$_4$Me-4, 1c; Y = NEt$_4$, R = Me, 1d) with HBF$_4$:Et$_2$O to afford products in which the alkylidyne groups do indeed migrate from the metal to the carborane cage. Thus, treatment of carbon monoxide saturated solutions of 1a or 1d with HBF$_4$·Et$_2$O gives the tetracarbonyl complexes [*closo*-1,2-Me$_2$-8-(CH$_2$R)-3,3,3,3-(CO)$_4$-3,1,2-WC$_2$B$_9$H$_8$] (R = C$_6$H$_4$Me-4, 4a; R = Me, 4b), while protonation in the presence of PhC$\equiv$CPh gives the alkyne complexes [*closo*-1,2-Me$_2$-8-(CH$_2$R)-3,3-(CO)$_2$-3,3-(η-PhC$_2$Ph)$_2$-3,1,2-WC$_2$B$_9$H$_8$] (R = C$_6$H$_4$Me-4, 5a; R = Me, 5b) which lose a CO ligand above ca. -20 °C, yielding the monocarbonyl species [*closo*-1,2-Me$_2$-8-(CH$_2$R)-3-(CO)-3,3-(η-PhC$_2$Ph)$_2$-3,1,2-WC$_2$B$_9$H$_8$]. Similarly, in the presence of PPh$_3$, protonation of 1a with HBF$_4$·Et$_2$O gives a mixture of the complexes [*closo*-1,2-Me$_2$-8-(CH$_2$R)-3,3-(CO)$_2$-3,3-(PPh$_3$)$_2$-3,1,2-WC$_2$B$_9$H$_8$] (6) and [*closo*-1,2-Me$_2$-8-(CH$_2$R)-3,3,3-(CO)$_3$-3-(PPh$_3$)-3,1,2-WC$_2$B$_9$H$_8$] (7), which equilibrate by disproportionation. In the presence of bidentate phosphines the initially formed alkylidene species can be intercepted to give ylide species of the type [*closo*-1,2-Me$_2$-3,3-(CO)$_2$-3-{CH(R)PPh$_2$-(CH$_2$)$_n$PPh$_2$}-3,1,2-WC$_2$B$_9$H$_9$] (R = C$_6$H$_4$Me-4, Me; n = 1, 2) (8).

All the products isolated so far from reactions of the salts 1 with HBF$_4$·Et$_2$O have carborane cages with adjacent CMe groups. In this paper we describe the results obtained by protonating the salts 1 and 2 with HCl and HI, affording products in which remarkably facile polytopal rearrangements of the CMe groups or eliminations of BH vertices from the carborane cages have occurred. Part of this work has been communicated.[7]

(6) Brew, S. A.; Devore, D. D.; Jenkins, P. D.; Pilotti, M. U.; Stone, F. G. A. *J. Chem. Soc., Dalton Trans.* 1992, 393.

(7) Brew, S. A.; Jeffery, J. C.; Pilotti, M. U.; Stone, F. G. A. *J. Am. Chem. Soc.* 1990, 112, 6148.

Chart I

	R	L
4a	C$_6$H$_4$Me-4	CO
4b	Me	CO
5a	C$_6$H$_4$Me-4	PhC$_2$Ph
5b	Me	PhC$_2$Ph
6	C$_6$H$_4$Me-4	PPh$_3$

7

8

	X	R	Y
9a	Cl	C$_6$H$_4$Me-4	NEt$_4$
9b	I	C$_6$H$_4$Me-4	N(PPh$_3$)$_2$
9c	I	C$_6$H$_4$Me-4	PPh$_4$
9d	I	Me	NEt$_4$

●CMe   ○BH   ⊕B

Results and Discussion

Treatment of a rapidly stirred CH$_2$Cl$_2$ solution of the salt [N(PPh$_3$)$_2$][*closo*-1,2-Me$_2$-3-($\equiv$CC$_6$H$_4$Me-4)-3,3-(CO)$_2$-3,1,2-WC$_2$B$_9$H$_9$] (1b) with ca. 1 mol equiv of aqueous HI afforded the complex [N(PPh$_3$)$_2$][*closo*-1,8-Me$_2$-11-(CH$_2$C$_6$H$_4$Me-4)-2-I-2,2,2-(CO)$_3$-2,1,8-WC$_2$B$_9$H$_8$] (9b). A similar reaction using the ethylidynetungsten complex [NEt$_4$][*closo*-1,2-Me$_2$-3-($\equiv$CMe)-3,3-(CO)$_2$-3,1,2-WC$_2$B$_9$H$_9$] (1d) gave [NEt$_4$][*closo*-1,8-Me$_2$-11-Et-2-I-2,2,2-(CO)$_3$-2,1,8-WC$_2$B$_9$H$_8$] (9d). The chloro analogue, [NEt$_4$][*closo*-1,8-Me$_2$-11-(CH$_2$C$_6$H$_4$Me-4)-2-Cl-2,2,2-(CO)$_3$-2,1,8-WC$_2$B$_9$H$_8$] (9a), was likewise prepared by reaction of the salt 1a with aqueous (or dry gaseous) HCl at ambient temperatures. In each case there was an immediate color change, and an IR spectrum measured less than 30 s after the addition of acid showed the reaction to be complete. When performed at -78 °C, the synthesis of 9b proceeded to completion within 10 min, successive IR measurements progressively indicating the course of the reaction.

Data characterizing the species 9a, 9b, and 9d are given in Tables I and II. Due to difficulty experienced in preparing powdered samples of complex 9b, its PPh$_4$$^+$ analogue 9c is described in the Experimental Section. Substitution of the cations in these salts produced no observable effect on the chemistry or spectroscopic behavior of their anions. It was immediately apparent from the NMR data that the salts 9 contain three carbonyl ligands and a BCH$_2$R (R = Me, C$_6$H$_4$Me-4) fragment. Thus, in the ^{1}H NMR spectrum of 9a the BCH$_2$C$_6$H$_4$Me-4 protons give

Table II. ^1H and $^{13}C\{^1H\}$ FT NMR Data[a]

compound	^1H (δ)	$^{13}C^b$ (δ)
9a	1.29 [t, 12 H, NCH$_2$Me, J(HH) 7], 1.56 (s, 3 H, CMe), 1.94 (s, 3 H, Me-4), 2.27 (s, 3 H, CMe), 2.30, 2.31 (m × 2, br, 2 H, BCH$_2$), 3.15 [q, 8 H, NCH$_2$Me, J(HH) 7], 6.85, 6.97 [(AB)$_2$, 4 H, C$_6$H$_4$, J(AB) 8]	236.0, 227.1, 225.4 (s × 3, WCO), 145.8 [C^1(C$_6$H$_4$)], 132.3 [C^4(C$_6$H$_4$)], 129.4 [C^2(C$_6$H$_4$)], 128.2 [C^3(C$_6$H$_4$)], 62.8 (CMe), 61.4 (br, CMe), 53.8 (NCH$_2$), 32.0 (v br, BCH$_2$), 31.4, 21.9 (CMe), 21.1 (Me-4), 7.9 (NCH$_2$Me)
9b	1.54, 1.89 (s × 2, 6 H, CMe), 2.19 (s, 3 H, Me-4), 2.40 (m br, 2 H, BCH$_2$), 6.84, 6.86 [(AB)$_2$, 4 H, C$_6$H$_4$, J(AB) 9], 7.45–7.68 (m, 30 H, Ph)	231.3 [WCO, J(WC) 124], 221.2, 220.8 [s × 2, WCO, J(WC) 65], 146.1 [C^1(C$_6$H$_4$)], 131.8 [C^4(C$_6$H$_4$)], 129.2 [C^3(C$_6$H$_4$)], 126.9 [C^2(C$_6$H$_4$)], 134.1–127.9 (m, Ph), 63.3 (CMe), 61.9 (br, CMe), 32.9, 29.5 (CMe), 32.1 [q, v br, BCH$_2$, J(BC) ca. 70], 21.9 (Me-4)
9d	0.81–0.95 (m br, 5 H, BCH$_2$Me), 1.35 [tt, 12 H, NCH$_2$Me, J(HH) 7, J(NH) 2], 1.64, 1.95 (s × 2, 6 H, CMe), 3.23 [q, 8 H, NCH$_2$, J(HH) 7]	231.1 [WCO, J(WC) 121], 221.8 [WCO, J(WC) 140], 221.2 [WCO, J(WC) 129], 62.4 (CMe), 61.9 (br, CMe), 53.2 (NCH$_2$), 32.8, 29.5 (CMe), 15.8 (v br, BCH$_2$), 15.2 (BCH$_2$Me), 7.9 (NCH$_2$Me)
10a	1.70, 1.74 (s × 2, 6 H, CMe), 2.14, 2.42 [(AB), 2 H, BCH$_2$, J(AB) 15], 2.26 (s, 3 H, Me-4), 6.92, 6.98 [(AB)$_2$, 4 H, C$_6$H$_4$, J(AB) 8]	210.2 [WCO, J(WC) 110], 143.0 [C^1(C$_6$H$_4$)], 134.3 [C^4(C$_6$H$_4$)], 129.0, 128.8 [C^{2,3}(C$_6$H$_4$)], 70.9 (CMe), 68.2 (br, CMe), 34.0 (CMe), 31.1 (v br, BCH$_2$), 29.4 (CMe), 21.0 (Me-4)
10b	0.81 (m, 3 H, BCH$_2$Me), 0.89 (m, 2 H, BCH$_2$), 1.72, 1.79 (s × 2, 6 H, CMe)	211.0 [WCO, J(WC) 112], 71.1 (CMe), 68.2 (br, CMe), 34.2, 29.6 (CMe), 16.1 [q, v br, BCH$_2$, J(BC) ca. 60], 14.9 (BCH$_2$Me)
11a	1.62, 1.78 (s × 2, 6 H, CMe), 2.17 (s, 3 H, Me-4), 1.88, 2.22 [(AB), 2 H, BCH$_2$, J(AB) 14], 6.56, 6.73 [(AB)$_2$, 4 H, C$_6$H$_4$, J(AB) 8], 7.19–7.49 (m, 10 H, Ph)	216.3 [WCO, J(WC) 147], 213.4 [WCO, J(WC) 160], 203.0 [PhC$_2$Ph, J(WC) 35], 142.4–128.3 (m, Ph and C$_6$H$_4$), 70.9 (CMe), 69.1 (br, CMe), 32.0, 34.6 (CMe), 30.5 [q, br, BCH$_2$, J(BC) 80], 14.2 (Me-4)
11b[c]	1.77, 1.78 (s × 2, 6 H, CMe), 2.19 (s, 3 H, Me-4), 2.68 (s, 3 H, ≡CMe), 6.45, 6.71 [(AB)$_2$, 4 H, C$_6$H$_4$, J(AB) 8], 7.54–7.65 (m, 5 H, Ph)	217.4, 214.5 (WCO), 207.2, 196.1 (PhC$_2$Me), 142.6, 136.6 [C^1(Ph and C$_6$H$_4$)], 133.1 [C^4(C$_6$H$_4$)], 130.9 [C^4(Ph)], 130.1, 129.5 [C^2(Ph and C$_6$H$_4$)], 128.6, 128.5 [C^3(Ph and C$_6$H$_4$)], 70.9 (CMe), 70.3 (br, CMe), 31.6, 29.1, 20.9, 20.2 [CMe, Me-4, PhC$_2$Me], 30.3 [q, v br, BCH$_2$, J(BC) ≈ 100]
12a	1.76 (s, 6 H, CMe), 7.43–7.67 (m, 30 H, Ph)	231.6 (WCO), 224.1 (2 WCO), 133.9 [C^4(Ph)], 132.3 [vt, C^2(Ph), |J(PC) + J(P′C)| 11], 129.6 [vt, C^3(Ph), |J(PC) + J(P′C)| 13], 127.2 [d, C^1(Ph), J(PC) 109], 64.5 (CMe), 31.2 (CMe)
12b	1.73 (s, 6 H, CMe), 7.45–7.65 (m, 30 H, Ph)	227.1 (WCO), 220.4 (2 WCO), 133.9 [C^4(Ph)], 132.3 [vt, C^2(Ph), |J(PC) + J(P′C)| 11], 129.6 [vt, C^3(Ph), |J(PC) + J(P′C)| 13], 127.2 [d, C^1(Ph), J(PC) 109], 64.9 (CMe), 32.5 (CMe)

[a] Chemical shifts (δ) in ppm, coupling constants in Hz, measurements at room temperature in CD$_2$Cl$_2$ unless otherwise stated. [b] Hydrogen-1 decoupled, chemical shifts are positive to high frequency of SiMe$_4$. [c] Peaks due to BCH$_2$ protons not observed.
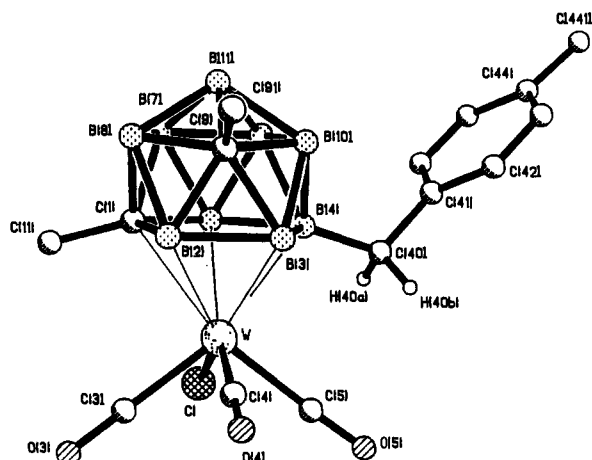

Figure 1. Structure of the anion of [NEt$_4$][closo-1,8-Me$_2$-11-(CH$_2$C$_6$H$_4$Me-4)-2-Cl-2,2,2-(CO)$_3$-2,1,8-WC$_2$B$_9$H$_8$] (**9a**), showing the crystallographic labeling scheme.

rise to two broad resonances at δ 2.30 and 2.31, each integrating to one proton. The corresponding signals in the spectrum of **9b** appear as a broad multiplet at δ 2.40, while the five protons of the BCH$_2$CH$_3$ group of **9d** give rise to a broad multiplet in the range δ 0.81–0.95. The related CH$_2$ signals in the $^{13}C\{^1H\}$ NMR spectra are observed as broad resonances at δ 32.0 (**9a**), 32.1 (**9b**), and 15.8 (**9d**). In accord with the data from the ^1H and ^{13}C NMR spectra, the $^{11}B\{^1H\}$ spectra (see the Experimental Section) all show a deshielded resonance (δ 4.1 (**9a**), 4.1 (**9b**), 5.0 (**9d**)) which remains a singlet in a fully coupled spectrum, due to the BCH$_2$R moieties. The structure of the salts **9** was not completely evident, however, until an X-ray diffraction study on [NEt$_4$][closo-1,8-Me$_2$-11-(CH$_2$C$_6$H$_4$Me-4)-2-Cl-2,2,2-(CO)$_3$-2,1,8-WC$_2$B$_9$H$_8$] (**9a**) had been carried out. Important bond lengths and angles are listed in Table III, and the anion is shown in Figure 1.

As expected, the tungsten atom is ligated on one side by three carbonyl groups (W–C(3) = 1.992 (8), W–C(4) = 1.975 (8), W–C(5) = 2.002 (9) Å) and a chlorine atom (W–Cl = 2.549 (2)

Table III. Selected Internuclear Distances (Å) and Angles (deg) for **9a**

W–Cl	2.549 (2)	C(3)–O(3)	1.160 (9)
C(4)–O(4)	1.13 (1)	C(5)–O(5)	1.13 (1)
C(1)–C(11)	1.53 (1)	B(2)–B(3)	1.83 (1)
B(4)–C(40)	1.62 (1)	B(4)–B(5)	1.79 (1)
C(1)–B(8)	1.73 (1)	B(2)–C(9)	1.695 (9)
B(3)–B(10)	1.756 (9)	B(4)–B(6)	1.78 (1)
B(5)–B(7)	1.77 (1)	B(7)–B(8)	1.74 (1)
C(9)–B(10)	1.697 (9)	B(6)–B(7)	1.75 (1)
B(8)–B(11)	1.75 (1)	B(10)–B(11)	1.76 (1)
W–C(3)	1.992 (8)	W–C(4)	1.975 (8)
W–C(5)	2.002 (9)	W–C(1)	2.395 (7)
C(1)–B(2)	1.70 (1)	B(3)–B(4)	1.790 (9)
C(40)–C(41)	1.502 (8)	B(5)–C(1)	1.721 (9)
B(8)–B(2)	1.78 (1)	C(9)–B(3)	1.72 (1)
B(10)–B(4)	1.77 (1)	B(6)–B(5)	1.77 (1)
B(7)–C(1)	1.732 (9)	B(8)–C(9)	1.69 (1)
B(10)–B(6)	1.74 (1)	B(7)–B(11)	1.74 (1)
C(9)–B(11)	1.720 (9)		
Cl–W–C(3)	75.1 (2)	W–C(4)–O(4)	179.0 (8)
C(3)–W–C(4)	75.7 (3)	W–B(4)–C(40)	113.5 (4)
W–C(3)–O(3)	179.6 (5)	Cl–W–C(5)	76.8 (3)
W–C(1)–C(11)	111.6 (4)	C(4)–W–C(5)	76.9 (4)
Cl–W–C(4)	134.0 (2)	W–C(5)–O(5)	177.7 (7)
C(3)–W–C(5)	104.2 (3)	B(4)–C(40)–C(41)	119.1 (5)

Å) and on the other side by the nido-icosahedral C$_2$B$_9$ fragment in the usual η^5 fashion. The most striking feature of the structure is that, unlike in the precursor alkylidyne complex **1a**, the cage CMe groups are no longer adjacent and are located in different pentagonal rings of the cage. Indeed, the framework of the cage has undergone a rearrangement which may be considered as a 120° clockwise rotation of the triangular face defined by the atoms labeled B(2)·C(9)·B(3). In addition, the CH$_2$C$_6$H$_4$Me-4 substituent is bonded to one of the boron atoms in the lower pentagonal ring (B(4)–C(40) = 1.62 (1) Å, B(4)–C(40)–C(41) = 119.1 (5)°). This is the boron atom that was in the β-position relative to the carbon atoms in the CCBBB ring of the starting complex **1a**, as is invariably the case in compounds containing this fragment.[4]

2206 *J. Am. Chem. Soc., Vol. 114, No. 6, 1992*

Brew et al.

Scheme I[a]

● CMe   ○ BH   ⊕ B
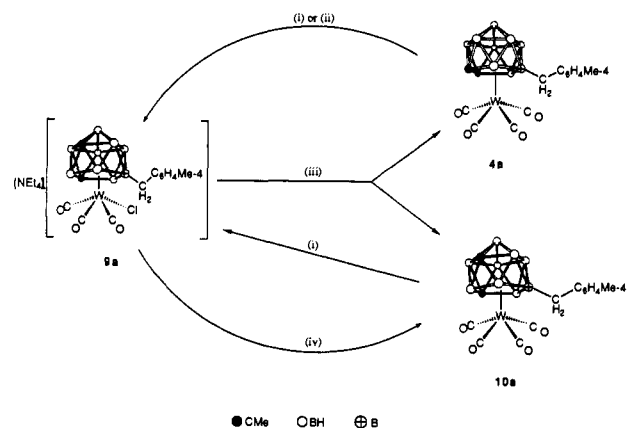
[a] Key: (i) NEt₄Cl (excess), THF, 5 days; (ii) NEt₄Cl (excess) THF, UV, 3 h; (iii) AgBF₄ (excess), CH₂Cl₂, gives 1:1 mixture of **4a** and **10a**; (iv) AgBF₄ (1 mol equiv), CH₂Cl₂.

The presence of the cage BCH₂R group was not unexpected in view of related studies on protonation reactions of the salts 1 in the presence of various Lewis bases (e.g., CO or PPh₃) and surely results from migration and insertion of the initially formed alkylidene fragment, CHR, into the B–H bond. That this process is accompanied by a cage framework rearrangement, however, is most surprising in view of the low temperatures (−78 °C) at which it readily occurs since such polytopal rearrangements in metallocarboranes, although not uncommon, generally require appreciably more forcing conditions.[8] Furthermore, reaction-induced rearrangements of this kind are rare. Hawthorne and co-workers[9] have previously observed a similar migration of a carbon vertex by treating the rhodacarborane complex [*exo-nido*-4,9-{(Ph₃P)₂Rh}-4,9-μ-(H)₂-7-Me-8-Ph-7,8-C₂B₉H₈] with excess PEt₃ to afford [*closo*-1-Me-2,2-(PEt₃)₂-2-H-8-Ph-2,1,8-RhC₂B₉H₉]. Although itself uncommonly facile, this process requires temperatures in excess of 50 °C. Thermal isomerization of tetracarbon–cobalt carboranes at room temperature has also been reported.[10]

The mechanism of the facile rearrangement of the CMe groups described herein is essentially unknown, but a number of reactions, which are summarized in Scheme I, have been undertaken in order to determine the conditions necessary to bring about the transformation with the hope of gaining an insight into how the process occurs. Thus, reaction of **4a** with NEt₄Cl in THF at ambient temperatures over a period of 5 days gave the compound [NEt₄][*closo*-1,8-Me₂-11-(CH₂R)-2-Cl-2,2,2-(CO)₃-2,1,8-WC₂B₉H₈] (R = C₆H₄Me-4) (**9a**), which was unambiguously shown to contain a rearranged cage by comparison of its NMR spectral parameters with those of authenticated samples of the salt **9a**. This observation demonstrates that the polytopal rearrangement and the migration of the alkylidene fragment into a B–H bond are independent processes. When the same reaction was performed in the presence of UV radiation, the salts **9** were again the only products isolated but the reaction was complete within 3 h. That the rate of rearrangement is greatly enhanced in this way suggests that, at least under these conditions, a dissociative mechanism is in operation. Remarkably, the process was also found to be reversible. Hence, treatment of a CO-saturated solution of **9c** with an excess of the reagent AgBF₄ afforded a 1:1 mixture of **4a**, which was identified by NMR spectroscopy, and the compound [*closo*-1,8-Me₂-11-(CH₂C₆H₄Me-4)-2,2,2,2-(CO)₄-2,1,8-WC₂B₉H₈] (**10a**). Similarly, a mixture of the compounds [*closo*-1,8-Me₂-11-Et-2,2,2,2-(CO)₄-2,1,8-WC₂B₉H₈] (**10b**) and **4b** was obtained from reaction of the salt **9d** with excess

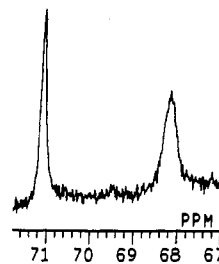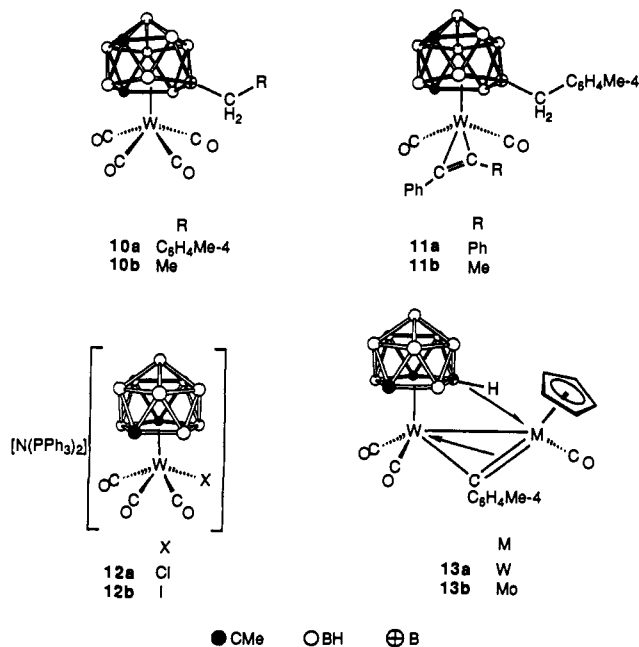(8) Hawthorne, M. F.; Callahan, K. P.; Wiersema, R. J. *Tetrahedron* **1974**, *30*, 1795.

(9) Knobler, C. B.; Marder, T. B.; Mizusawa, E. A.; Teller, R. G.; Long, J. A.; Behnken, P. E.; Hawthorne, M. F. *J. Am. Chem. Soc.* **1984**, *106*, 2990.

(10) Wang, Z. T.; Sinn, E.; Grimes, R. N. *Inorg. Chem.* **1985**, *24*, 826.

Figure 2. ¹³C{¹H} NMR spectrum of **10b** showing the *C*Me resonances.

Chart II

R

	R
10a	C₆H₄Me-4
10b	Me

	R
11a	Ph
11b	Me

[N(PPh₃)₂]

	X
12a	Cl
12b	I

	M
13a	W
13b	Mo

● CMe   ○ BH   ⊕ B

AgBF₄. Data characterizing the new compounds **10a** and **10b** are collected in Tables I and II and are entirely consistent with these compounds being isomers, containing rearranged C₂B₉ cages, of **4a** and **4b**. Thus, in the ¹H NMR spectrum, the protons of the BCH₂R group are seen (Table II) as either an AB-type pattern (**10a**) or a broad unresolved multiplet (**10b**). The ¹¹B NMR data (Experimental Section) confirm the presence of this group with resonances at δ 6.3 and 6.9 for **10a** and **10b**, respectively. That the cage CMe groups are not adjacent in **10a** and **10b** is demonstrated in Figure 2, which shows the ¹³C{¹H} NMR spectrum of **10b** in the region where the signals due to the cage *C*Me nuclei appear. The observation of two resonances establishes that the compounds **10** do not contain a plane of symmetry between the *C*Me groups like the one present in **4a** and **4b**.[6] Moreover, we have found that for compounds in which the two *C*Me groups are not adjacent and occupy vertices in different pentagonal rings of the cage, one resonance consistently appears much broader than the other. This is in contrast with those compounds containing two nonequivalent *C*Me groups that occupy vertices adjacent to the tungsten atom, for which the *C*Me signals are of comparable width. Since both compounds **10a** and **10b** show one broad and one relatively sharp resonance for the *C*Me nuclei in their ¹³C{¹H} NMR spectra (Figure 2), they can be assigned a structure in which the carborane cage system has nonadjacent *C*Me groups which occupy sites in different pentagonal rings of the cage. Obviously the relative line widths of the signals due to the *C*Me nuclei cannot alone be taken as absolute proof that the cage has the topology of that in compound **9a**. However, when considered alongside the other spectroscopic data we have found this to be a powerful and reliable indicator of the relative positions of the cage CMe groups.

Interestingly, the reaction between the salts **9** and 1 mol equiv of AgBF₄ in the presence of CO gave only the compounds **10**, in
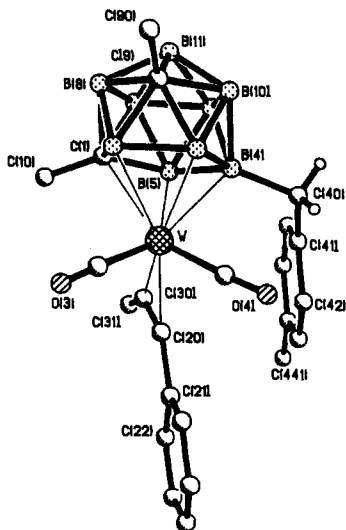
Figure 3. Molecular structure of [*closo*-1,8-Me$_2$-11-(CH$_2$C$_6$H$_4$Me-4)-2,2-(CO)$_2$-2-(η-PhCCMe)-2,1,8-WC$_2$B$_9$H$_8$] (**11b**), showing the crystallographic labeling scheme.

which the cage CMe groups remain separated. It should be noted that addition of NEt$_4$Cl to THF solutions of the tetracarbonyl species **10** simply yielded the salts **9** and did not lead to a product in which a second polytopal rearrangement had occurred.

Clearly a unique unequivocal mechanism for the cage isomerization process cannot account for all the observations described. However, with the limited amount of data available, the most plausible explanation for the formation of the salts **9** from the compounds **1** would involve protonation of the alkylidyne complex to give an alkylidene species which undergoes migration and insertion of the alkylidene fragment into a B–H bond. Scavenging of CO would then give a tetracarbonyl species. Indeed, this process is known to occur readily at −78 °C if protonation is carried out with HBF$_4$·Et$_2$O in the presence of CO.[6] Attack at the metal center by the halide ion could then lead to a nido-12-vertex tungstacarborane species, with a formally satisfied 14 polyhedral skeletal electronic-pair count, which would be free to undergo cage rearrangement through diamond–square–diamond processes resulting in the rotation of a triangular face of the cage containing a carbon and two boron atoms. Closure of the nido intermediate and elimination of CO would then yield the observed products. The involvement of such a 12-vertex nido intermediate in the isomerization of *o*-carborane (1,2-C$_2$B$_{10}$H$_{12}$) to *m*-carborane (1,7-C$_2$B$_{10}$H$_{12}$) was recently postulated by Edvenson and Gaines.[11]

Compounds **9** are proving to be useful reagents for further syntheses. Hence, treatment of **9c** in CH$_2$Cl$_2$ with the alkynes PhC≡CR′ (R′ = Me, Ph) followed by portionwise addition of AgBF$_4$ afforded the purple complexes [*closo*-1,8-Me$_2$-11-(CH$_2$C$_6$H$_4$Me-4)-2-(η-PhC$_2$R′)-2,2-(CO)$_2$-2,1,8-WC$_2$B$_9$H$_8$] (R′ = Ph, **11a**; R′ = Me, **11b**) in high yield. Data characterizing these complexes are given in Tables I and II, but discussion of the spectroscopic properties is deferred until the results of an X-ray diffraction study on complex **11b** have been described. Selected bond lengths and angles are listed in Table IV, and the molecular structure is shown in Figure 3.

As expected, the tungsten atom is coordinated by two CO groups (W–C(3) = 2.010 (4), W–C(4) = 1.972 (5) Å) and an alkyne molecule which is bound in the normal η^2 fashion (W–C(20) = 2.083 (5), W–C(30) = 2.047 (5), C(20)–C(30) = 1.314 (5) Å), with the Ph and Me groups bent away from the metal center (W–C(20)–C(21) = 149.0 (3), W–C(30)–C(31) = 147.8 (4)°). The parameters for the coordinated alkyne may be compared to those in the compound [W{=C(H)Ph}Cl$_2$(η-C$_2$Ph$_2$)-(PMe$_3$)$_2$][12] (W—C = 2.061 (7), 2.04 (2) Å, C=C = 1.33 (3) Å).

(11) Edvenson, G. M.; Gaines, D. F. *Inorg. Chem.* **1990**, *29*, 1210.
(12) Mayr, A.; Lee, K. S.; Kjelsberg, M. A.; Ergen, D. V. *J. Am. Chem. Soc.* **1986**, *108*, 6079.

Table IV. Selected Internuclear Distances (Å) and Angles (deg) for **11b**

W–C(3)	2.010 (4)	B(8)–C(9)	1.709 (8)
W–C(20)	2.083 (5)	C(3)–O(3)	1.129 (6)
C(30)–C(31)	1.485 (7)	C(20)–C(21)	1.457 (6)
W–B(4)	2.359 (5)	W–B(2)	2.369 (6)
C(1)–B(5)	1.722 (6)	C(1)–C(10)	1.519 (7)
B(2)–B(8)	1.779 (7)	C(1)–B(8)	1.694 (9)
B(3)–B(10)	1.765 (7)	B(3)–B(4)	1.827 (7)
B(4)–C(40)	1.621 (7)	B(4)–B(6)	1.813 (6)
B(6)–B(10)	1.759 (8)	B(5)–B(7)	1.774 (7)
B(8)–B(11)	1.765 (8)	B(7)–B(8)	1.740 (8)
C(9)–B(10)	1.702 (7)	B(10)–B(11)	1.755 (8)
W–C(4)	1.972 (5)	C(4)–O(4)	1.141 (6)
W–C(30)	2.047 (5)	C(20)–C(30)	1.314 (5)
W–C(1)	2.411 (4)	W–B(3)	2.394 (7)
W–B(5)	2.368 (4)	C(1)–B(2)	1.704 (7)
C(1)–B(7)	1.724 (6)	B(2)–B(3)	1.792 (8)
B(2)–C(9)	1.725 (8)	B(3)–C(9)	1.712 (8)
B(4)–B(5)	1.844 (7)	B(4)–B(10)	1.793 (9)
B(5)–B(6)	1.775 (8)	B(6)–B(7)	1.758 (7)
B(6)–B(11)	1.743 (9)	B(7)–B(11)	1.75 (1)
C(9)–B(11)	1.717 (7)	C(9)–C(90)	1.517 (9)
W–C(3)–O(3)	177.7 (6)	B(4)–C(40)–C(41)	114.5 (4)
C(3)–W–C(20)	84.7 (2)	W–C(30)–C(20)	73.0 (3)
C(4)–W–C(30)	111.5 (2)	C(20)–C(30)–C(31)	139.1 (5)
W–B(4)–C(40)	114.7 (3)	C(3)–W–C(4)	83.8 (2)
W–C(20)–C(30)	69.9 (3)	C(4)–W–C(20)	78.5 (2)
C(21)–C(20)–C(30)	141.0 (5)	W–C(1)–C(10)	109.4 (3)
W–C(4)–O(4)	176.9 (4)	W–C(20)–C(21)	149.0 (3)
C(3)–W–C(30)	104.4 (2)	W–C(30)–C(31)	147.8 (4)
C(20)–W–C(30)	37.1 (2)		

The WC$_2$B$_9$H$_8$(CH$_2$C$_6$H$_4$Me-4) icosahedron clearly shows CMe groups having the same disposition as in **9a**.

The ^{1}H, ^{13}C, and ^{11}B NMR spectral data for the compounds **11** are in agreement with the solid-state structure established for **11b**. In the ^{1}H NMR spectrum of **11a**, an AB-type pattern is seen at δ 1.88 and 2.22 due to the BC*H*$_2$C$_6$H$_4$Me-4 protons. The corresponding signals in the spectrum of **11b** are not observed, presumably due to coincidence with other resonances, but the presence of the BCH$_2$Me fragment is confirmed by the observation of a deshielded resonance at δ 11.1 in the ^{11}B NMR spectrum and by a quartet resonance at δ 30.3 in the ^{13}C{^{1}H} spectrum due to the BCH$_2$Me nucleus. For **11a**, the corresponding signals are seen at δ 11.2 and 30.5, respectively. In order for the tungsten atom to achieve a filled 18-electron valence shell, the alkyne must denote 4 electrons to the metal. This is borne out by resonance of the ligated carbon atoms (δ 203.0, **11a**; 207.2 and 196.1, **11b**) in the range normally associated with 4-electron-donor alkyne ligands.[13]

In accord with a structure in which the cage CMe groups are located in different pentagonal rings, both **11a** and **11b** show two resonances for the cage *C*Me nuclei in their ^{13}C{^{1}H} NMR spectra (δ 70.9 and 69.1, **11a**; 70.9 and 70.3, **11b**), one appearing much broader than the other in each case. Further reactions of the salts **9** have been undertaken, with results to be published elsewhere.

Having uncovered such a facile rearrangement of the 12-vertex closed polyhedron present in the salts **1**, it was important to investigate protonation reactions of the salt [N(PPh$_3$)$_2$][*closo*-1,6-Me$_2$-4-(≡CC$_6$H$_4$Me-4)-4,4-(CO)$_2$-4,1,6-WC$_2$B$_{10}$H$_{10}$] (**2**), which contains a 13-vertex cage system.

Reaction of **2** with HX in CH$_2$Cl$_2$ was markedly slower than the protonations of the salts **1** described above and afforded the orange salts [N(PPh$_3$)$_2$][*closo*-1,7-Me$_2$-2-X-2,2,2-(CO$_3$)-2,1,7-WC$_2$B$_9$H$_9$] (X = Cl, **12a**; X = I, **12b**) overnight. It was immediately apparent from the spectroscopic data for compounds **12a** and **12b** (Tables I and II and Experimental Section) that the CC$_6$H$_4$Me-4 fragment present in the precursor alkylidyne complex had been lost and, furthermore, that the η^6-C$_2$B$_{10}$H$_{10}$Me$_2$ cage system was no longer present. Both **12a** and **12b** showed three CO absorptions in their IR spectra (Table I), and correspondingly, signals due to three CO groups were observed in their ^{13}C{^{1}H}

(13) Templeton, J. L. *Adv. Organomet. Chem.* **1989**, *29*, 1.

2208 *J. Am. Chem. Soc., Vol. 114, No. 6, 1992*

Brew et al.

Table V. Selected Internuclear Distances (Å) and Angles (deg) for **12b**

W–I	2.899 (2)	B(10)–B(11)	1.76 (2)
C(6)–O(6)	1.15 (1)	C(5)–O(5)	1.17 (1)
C(1)–C(3)	1.53 (1)	C(7)–O(7)	1.15 (1)
W–B(4)	2.357 (9)	W–C(2)	2.400 (8)
C(1)–B(8)	1.68 (2)	B(5)–B(7)	1.78 (1)
C(2)–B(10)	1.73 (1)	B(3)–B(9)	1.74 (2)
B(6)–B(7)	1.77 (2)	B(4)–B(6)	1.75 (1)
B(10)–B(6)	1.76 (2)	B(8)–B(9)	1.75 (2)
B(9)–B(11)	1.75 (1)	B(7)–B(11)	1.75 (2)
W–C(5)	1.97 (1)	W–C(6)	1.973 (8)
W–C(7)	1.963 (9)	W–C(1)	2.455 (8)
W–B(3)	2.39 (1)	C(2)–C(4)	1.55 (1)
W–B(5)	2.372 (9)	B(7)–C(1)	1.73 (1)
B(8)–B(3)	1.75 (1)	B(9)–C(2)	1.72 (1)
B(10)–B(4)	1.78 (1)	B(6)–B(5)	1.78 (1)
B(7)–B(8)	1.77 (2)	B(9)–B(10)	1.76 (2)
B(6)–B(11)	1.80 (2)	B(8)–B(11)	1.75 (2)
I–W–C(7)	131.0 (2)	W–C(2)–C(4)	108.8 (5)
C(5)–W–C(6)	102.0 (4)	I–W–C(5)	74.9 (3)
W–C(1)–C(3)	108.5 (6)	C(6)–W–C(7)	75.4 (3)
I–W–C(2)	98.5 (2)	I–W–C(1)	108.3 (2)
I–W–C(6)	74.7 (2)		
C(5)–W–C(7)	74.8 (3)		
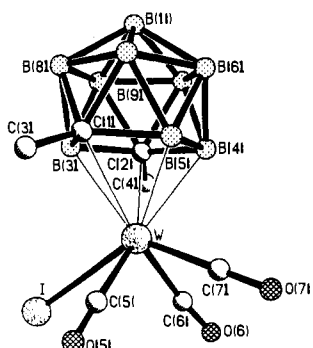
Figure 4. Structure of the anion of [N(PPh₃)₂][*closo*-1,7-Me₂-2-I-2,2,2-(CO)₃-2,1,7-WC₂B₉H₉] (**12b**), showing the crystallographic labeling scheme.

NMR spectra (Table II), the only other resonances in the ¹³C{¹H} NMR spectrum, apart from those assigned to the N(PPh₃)₂⁺ cation, being due to cage CMe groups. In accord with this, the ¹H NMR spectrum showed only signals arising from the cage CMe protons and the countercation (Table II). Most revealing of all, the ¹¹B NMR spectra of **12a** and **12b** (Experimental Section) each showed six resonances in a 1:2:2:1:2:1 ratio corresponding to only nine boron atoms. In order to fully characterize these compounds, an X-ray diffraction study was carried out on **12b**. The results are summarized in Table V, and the structure is shown in Figure 4.

The anion of **12b** consists of a tungsten atom ligated by three CO groups (W–C(5) = 1.97 (1), W–C(6) = 1.973 (8), W–C(7) = 1.963 (9) Å), an iodine atom (W–I = 2.899 (2) Å), and an η⁵ C₂B₉H₉ cage system. Thus, the docosahedral WC₂B₁₀ framework in the starting complex **2** has been transformed to icosahedral WC₂B₉ geometry. The lower pentagonal ring of this icosahedron has a CBCBB arrangement of atoms. We have observed this topology previously in compounds **13a** and **13b**, which were also formed from the salts **2** via a cage degradation process brought about by protonation with HBF₄·Et₂O in the presence of [M(≡CC₆H₄Me-4)(CO)₂(η-C₅H₅)] (M = Mo, W).[3a]

The formation of **12a** and **12b** involves the loss of a BH vertex as well as the alkylidene fragment C(H)C₆H₄Me-4. It would be unwise to suggest a mechanism for the loss of these fragments on the basis of the available data, but in view of the results obtained from protonation reactions of the salts **1**, it seems likely that protonation would initially give an alkylidene species. If the alkylidene fragment were then to migrate and insert into a B–H bond of the cage, the strain inherent in the C₂B₁₀H₁₀ framework

could be the driving force for the expulsion of a B(H)C(H)C₆H₄Me-4 fragment, possibly as HB=C(H)C₆H₄Me-4. Whatever the mechanism, it is becoming increasingly apparent that the process is extremely facile and is one that the salts **2** frequently follow in their reaction chemistry. It is noteworthy that degradation of 13-vertex to 12-vertex CoC₄B₇ cages under acidic conditions has been observed.[14]

Conclusions

The work described in this paper further highlights the diverse nature of the species obtainable through reactions of the salts **1** and **2**. The observed separation of cage CMe groups occurs at unprecedentedly low temperatures and was totally unexpected. Why the barrier to rearrangement should be so low in these systems is, at the present time, puzzling and clearly warrants further study. The reversible character of this isomerization (**4** ↔ **9**) is, to the best of our knowledge, the first example of such a process for a metallacarborane, since separation of the carbon atom vertices of these cage systems generally leads to a thermodynamically more stable product. Only one other example of reverible cage isomerization is known to us, namely the conversion of 1,7-C₂B₁₀H₁₂ to 1,2-C₂B₁₀H₁₂ via 2-electron reduction with sodium metal.[15] That an increase of negative charge in the cage might remove the thermodynamic preference for separated carbon vertices was predicted by Hoffmann and Lipscomb,[16] and such considerations may also be relevant to this work. Much further work is likely to be required, however, before these processes receive a satisfactory explanation. Although not totally unexpected in view of previous results obtained in this laboratory, the expulsion of a BH vertex from the MC₂B₁₀H₁₀ cage system is a remarkable phenomenon in view of the acidic reaction conditions under which it occurs.

Experimental Section

Petroleum ether refers to that fraction of bp 40–60 °C. Experiments were carried out using Schlenk-tube techniques under a dry nitrogen atmosphere, and all solvents were rigorously dried before use. Alumina (Aldrich, Brockmann activity III), silica (Fluka, Kieselgel 70–230 mesh), and Florisil (Aldrich, 100–200 mesh) were used for chromatography employing water-jacketed columns of given dimensions at ca. 10 °C, unless otherwise stated. The salts **1** were prepared as previously reported,[17] and the salt **2** was prepared from [W(≡CC₆H₄Me-4)-(CF₃CO₂)(CO)₂(NC₅H₄Me-4)₂] by the method previously described for the NEt₄ salt,[18] using N(PPh₃)₂Cl in place of NEt₄Cl. Hydrochloric and hydroiodic acids were used as aqueous solutions, of 36% and 57% concentrations, respectively (except where otherwise stated). The NMR spectra were recorded with JEOL JNM GX270 and GX400 spectrometers, and the IR spectra were obtained with a Perkin-Elmer FT1600 spectrometer. Boron-11 NMR data are recorded with chemical shifts (δ) in ppm, measurements in CD₂Cl₂ at ambient temperature. All are hydrogen-1 decoupled, and chemical shifts are positive to high frequency of BF₃·Et₂O (external).

Synthesis of [NEt₄][*closo*-1,8-Me₂-11-(CH₂C₆H₄Me-4)-2-Cl-2,2,2-(CO)₃-2,1,8-WC₂B₉H₈] (**9a**). A CH₂Cl₂ (20 mL) solution of **1a** (0.11 g, 0.17 mmol) was stirred rapidly at room temperature and treated dropwise with 1 equiv of aqueous HCl. An immediate color change from orange to brown was observed, and an IR spectrum of the mixture showed the reaction was complete within 30 s. Solvent volume was reduced in vacuo to ca. 3 mL, for chromatography on alumina (3 × 5 cm column) at −30 °C. Elution of the column with CH₂Cl₂ afforded an orange band which was collected and from which solvent was removed in vacuo. Recrystallization of the residue by slow diffusion of Et₂O (5 mL) into a THF solution (2 mL) at 0 °C afforded yellow crystals of **9a** (0.055 g). ¹¹B{¹H} NMR: δ 4.1 (s, 1 B, BCH₂), 0.6, −4.3, −5.4, −7.1, −10.0, −11.5, −12.3, −15.2 (1 B × 8).

Synthesis of [PPh₄][*closo*-1,8-Me₂-11-(CH₂C₆H₄Me-4)-2-I-2,2,2-(CO)₃-2,1,8-WC₂B₉H₈] (**9c**). A CH₂Cl₂ (20 mL) solution of **1c** (1.00 g,

(14) Maxwell, W. M.; Grimes, R. N. *Inorg. Chem.* **1979**, *18*, 2174.
(15) Zakharin, L. I.; Kalinin, V. N.; Podvisotskaya, L. S. *Bull. Acad. Sci. U.S.S.R. Chem. Sci.* **1967**, 2212.
(16) Hoffmann, R.; Lipscomb, W. N. *Inorg. Chem.* **1963**, *2*, 231.
(17) (a) Baumann, F.-E; Howard, J. A. K.; Johnson, O.; Stone, F. G. A. *J. Chem. Soc., Dalton Trans.* **1987**, 2661. (b) Green, M.; Howard, J. A. K.; James, A. P.; Nunn, C. M.; Stone, F. G. A. *J. Chem. Soc., Dalton Trans.* **1987**, 61.
(18) Crennell, S. J.; Devore, D. D.; Henderson, S. J. B.; Howard, J. A. K.; Stone, F. G. A. *J. Chem. Soc., Dalton Trans.* **1989**, 1363.

Table VI. Crystallographic Data for **9a**, **11b**, and **12b**[a]

	9a	11b	12b
formula	$C_{23}H_{46}B_9ClNO_3W \cdot 0.5C_4H_8O$	$C_{23}H_{31}B_9O_2W$	$C_{43}H_{45}B_9INO_3P_2W$
fw	737.3	620.6	1093.8
crystal color, shape	orange rhombs	purple prisms	orange plates
crystal dimens, mm	$0.1 \times 0.2 \times 0.6$	$0.5 \times 0.5 \times 0.7$	$0.2 \times 0.3 \times 0.3$
crystal system	triclinic	triclinic	monoclinic
space group (no.)	$P\bar{1}$ (2)	$P\bar{1}$ (2)	$P2_1/c$ (14)
a, Å	9.939 (4)	8.092 (2)	10.720 (2)
b, Å	11.974 (6)	11.019 (3)	13.382 (3)
c, Å	14.108 (6)	16.055 (5)	31.973 (6)
α, deg	96.41 (4)	73.89 (2)	
β, deg	90.43 (3)	75.40 (2)	90.46 (2)
γ, deg	99.27 (3)	84.61 (2)	
V, Å^3	1646 (1)	1331 (1)	4587 (2)
Z	2	2	4
d_{calcd}, g cm^{-3}	1.49	1.55	1.58
μ(Mo Kα), cm^{-1}	36.9	44.5	33.5
$F(000)$, e	742	608	2144
2θ range, deg	3–50	3–50	4–50
no. of unique reflcns	5818	5056	8076
no. of obsd reflcns	4949	4694	5158
criterion for obsd n $[F_o \geq n\sigma(F_o)]$	$n = 5$	$n = 6$	$n = 5$
R $(R')^b$	0.036 (0.036)	0.023 (0.025)	0.036 (0.035)
final electron density diff features (max/min), e Å^{-3}	1.20/−0.57	0.62/−0.74	0.61/−0.63

[a] Data collected at 298 K on a Siemens R3m/V automated diffractometer operating in the θ–2θ scan mode; graphite monochromated Mo Kα X-radiation, $\bar{\lambda} = 0.71069$ Å. Refinement was by full matrix least squares with a weighting scheme of the form $w^{-1} = [\sigma^2(F_o) + g|F_o|^2]$ with $g = 0.00055$ (**9a**), 0.00045 (**11b**), 0.00050 (**12b**); $\sigma^2(F_o)$ is the variance in F_o due to counting statistics; g was chosen so as to minimize variation in $\sum w(|F_o| - |F_c|)^2$ with $|F_o|$. [b] $R = \sum||F_o| - |F_c||/\sum|F_o|$, $R' = \sum w^{1/2}||F_o| - |F_c||/\sum w^{1/2}|F_o|$.

1.19 mmol) was stirred rapidly at −78 °C and treated dropwise with 1 equiv of aqueous HI. Successive IR measurements progressively indicated the course of the reaction, which was complete within 10 min. The mixture was warmed to room temperature and solvent volume reduced in vacuo to ca. 3 mL, for chromatography on alumina (3 × 10 cm column) at −30 °C. Elution of the column with CH_2Cl_2 afforded an orange band which was collected and from which solvent was removed in vacuo. Recrystallization of the residue from CH_2Cl_2/Et_2O (10 mL, 1:20) with vigorous stirring afforded orange microcrystals of **9c** (0.56 g). $^{11}B\{^1H\}$ NMR of **9b**: δ 4.1 (s, 1 B, BCH$_2$), −4.2 (br, 3 B), −8.2 (1 B), −10.9 (2 B), −12.9, −16.2 (1 B × 2).

Synthesis of [NEt$_4$][*closo*-1,8-Me$_2$-11-Et-2-I-2,2,2-(CO)$_3$-2,1,8-WC$_2$B$_9$H$_8$] (9d). A CH_2Cl_2 (20 mL) solution of **1d** (0.11 g, 0.36 mmol) was stirred rapidly at room temperature and treated dropwise with 1 equiv of aqueous HI. An immediate color change from yellow to brown occurred, and an IR spectrum of the mixture showed the reaction was complete within 30 s. Solvent volume was reduced in vacuo to ca. 3 mL, for chromatography on alumina (3 × 10 cm column) at −30 °C. Elution of the column with CH_2Cl_2 afforded an orange band which was collected and from which solvent was removed in vacuo. Recrystallization of the residue from CH_2Cl_2/Et_2O (10 mL, 1:20) with vigorous stirring afforded ochre microcrystals of **9d** (0.10 g). $^{11}B\{^1H\}$ NMR: δ 5.0 (s, 1 B, BCH$_2$), −4.2 (2 B), −4.9, −7.7, −10.0, −11.2, −12.9, −16.8 (1 B × 6).

Synthesis of [*closo*-1,8-Me$_2$-11-(CH$_2$C$_6$H$_4$Me-4)-2,2,2,2-(CO)$_4$-2,1,8-WC$_2$B$_9$H$_8$] (10a). A stream of dry CO gas was passed through a solution of **9c** (0.20 g, 0.20 mmol) in CH_2Cl_2 (20 mL) for 10 min. This saturated solution was then treated with AgBF$_4$ (40 mg, 0.20 mmol) and stirred for 30 min until the reaction was complete (IR), all the while maintaining a gentle flow of CO through the mixture. After removal of the solvent in vacuo, Et$_2$O (3 mL) was added and the resulting slurry transferred to a chromatography column packed with Florisil (2 × 12 cm). Elution of the column at −40 °C with Et$_2$O afforded a yellow band which, after removal of solvent in vacuo to ca. 4 mL and cooling to −78 °C, yielded yellow microcrystals of **10a** (0.11 g). $^{11}B\{^1H\}$ NMR: δ 6.3 (s, 1 B, BCH$_2$), 1.5, −4.3, −5.7 (1 B × 3), −7.1 (2 B), −11.9, −12.2, −15.5 (1 B × 3).

Synthesis of [*closo*-1,8-Me$_2$-11-Et-2,2,2,2-(CO)$_4$-2,1,8-WC$_2$B$_9$H$_8$] (10b). A similar preparation to that described for **10a** above, starting from **9d** (0.07 g, 0.10 mmol) and treating with CO and AgBF$_4$ (20 mg, 0.10 mmol) gave, after workup as described for **10a**, yellow microcrystals of **10b** (0.04 g). $^{11}B\{^1H\}$ NMR: δ 6.9 (s, 1 B, BCH$_2$), 1.4, −4.8, −6.3 (1 B × 3), −7.3, −11.9 (2 B × 2), −16.0 (1 B).

Synthesis of [*closo*-1,8-Me$_2$-11-(CH$_2$C$_6$H$_4$Me-4)-2-(η-PhC$_2$Ph)-2,2-(CO)$_2$-2,1,8-WC$_2$B$_9$H$_8$] (11a). The reagents **9c** (0.20 g, 0.20 mmol) and PhC≡CPh (0.15 g, 0.84 mmol) were mixed and dissolved in CH_2Cl_2 (15 mL). Addition of AgBF$_4$ (40 mg, 0.20 mmol) in small portions until the reaction was complete (IR) gave a dark mixture. The solvent was removed in vacuo and n-hexane (2 mL) added. The resulting slurry was transferred via a syringe to a chromatography column (alumina, 2 × 15

cm), from which a purple fraction was then eluted with n-hexane. Reduction of the volume of this eluate to ca. 3 mL by removal of solvent in vacuo, followed by cooling to −20 °C, afforded purple crystals of **11a** (0.11 g). $^{11}B\{^1H\}$ NMR: δ 11.2 (s, 1 B, BCH$_2$), −1.2 (2 B), −2.3, −5.9, −7.8, −11.2, −12.8, −13.7 (1 B × 6).

Synthesis of [*closo*-1,8-Me$_2$-11-(CH$_2$C$_6$H$_4$Me-4)-2-(η-MeC$_2$Ph)-2,2-(CO)$_2$-2,1,8-WC$_2$B$_9$H$_8$] (11b). A similar synthesis employing **9c** (0.20 g, 0.20 mmol), MeC≡CPh (0.10 g, 8.86 mmol), and AgBF$_4$ (40 mg, 0.20 mmol) led to the isolation of purple microcrystals of **11b** (0.12 g). $^{11}B\{^1H\}$ NMR: δ 11.1 (s, 1 B, BCH$_2$), −1.2 to −13.1 (br, 8 B).

Synthesis of [N(PPh$_3$)$_2$][*closo*-1,7-Me$_2$-2-Cl-2,2,2-(CO)$_3$-2,1,7-WC$_2$B$_9$H$_9$] (12a). Aqueous HCl (1 mL of a 0.33 M solution) was added to a solution of **2** (0.25 g, 0.24 mmol) in CH_2Cl_2 (25 mL), and the resulting mixture was vigorously stirred for 16 h. After this time the solvent was evaporated and the residue dried in vacuo for 2 h. The residue was then redissolved in CH_2Cl_2 (30 mL), adsorbed onto Kieselgel (ca. 3 g), and transferred to the top of a Kieselgel chromatography column (2 × 15 cm) at −20 °C. Elution with CH_2Cl_2 gave a yellow eluate from which orange microcrystals of **12a** were obtained (0.11 g) by reducing the volume of the solvent to ca. 5 mL in vacuo and adding petroleum ether (10 mL). $^{11}B\{^1H\}$ NMR: δ −6.5 (1 B), −8.7, −9.8 (2 B × 2), −11.3 (1 B), −13.2 (2 B), −13.8 (1 B).

Synthesis of [N(PPh$_3$)$_2$][*closo*-1,7-Me$_2$-2-I-2,2,2-(CO)$_3$-2,1,7-WC$_2$B$_9$H$_9$] (12b). To a rapidly stirred solution of **2** (0.37 g, 0.35 mmol) in CH_2Cl_2 (25 mL) was added aqueous HI (10 drops), and stirring of the resulting mixture continued for 12 h. Solvent was removed and the residue dried in vacuo for 2 h before being redissolved in CH_2Cl_2 (20 mL), adsorbed onto Kieselgel (ca. 3 g), and transferred to the top of a Kieselgel chromatography column (2 × 15 cm) at −20 °C. Elution with CH_2Cl_2/petroleum ether (2:1) removed a yellow fraction from which removal of solvent in vacuo gave **12b** as an orange powder (0.18 g). $^{11}B\{^1H\}$ NMR: δ −6.8 (1 B), −8.8, −10.3 (2 B × 2), −11.5 (1 B), −13.1 (2 B), −14.2 (1 B).

Polytopal Rearrangement by Chloride Substitution. A mixture of compound **4a** (0.050 g, 0.089 mmol) and NEt$_4$Cl·H$_2$O (0.15 g, 0.90 mmol) was dissolved in THF (10 mL) and stirred for 5 days. After removal of the solvent in vacuo, CH_2Cl_2 (2 mL) was added to the mixture and the resultant slurry worked up as described for synthesis of **9a** above. Yellow microcrystals of **9a** (0.048 g, 96% yield) were thus obtained.

It was found that the same result could be achieved by UV irradiation (250-W mercury lamp) of the reaction mixture, prepared in the same way, in a water-cooled jacketed Schlenk flask. Within 3 h the reaction was complete (IR), and workup as described above yielded yellow microcrystals of **9a** (0.041 g, 82% yield).

Any possible significance of water of crystallization in the chloride salts used for these reactions was ruled out by replacement of NEt$_4$Cl·H$_2$O with dry PPh$_4$Cl (0.34 g, 0.90 mmol). Following identical procedures to those described above, essentially unaltered yields of the PPh$_4{}^+$ analogue of **9a** were obtained.

A mixture of **10a** (0.050 g, 0.089 mmol) and NEt₄Cl·H₂O (0.15 g, 0.90 mmol) was dissolved in THF (10 mL) and stirred for 5 days. Workup as described above yielded yellow microcrystals of **9a** (0.045 g, 90% yield).

Reverse Isomerization Reactions. A CH₂Cl₂ (20 mL) solution of **9c** (0.20 g, 0.20 mmol) was treated with CO gas, as described for the synthesis of compounds **10** above. Once the solution was saturated with the gas, a single portion of AgBF₄ (0.10 g, 0.50 mmol) was added and a slow stream of CO maintained for 30 min until the reaction was complete (IR). Solvent was removed in vacuo and Et₂O (2 mL) added to the residue for transfer to the top of a Florisil-packed chromatography column (2 × 18 cm). Elution at –40 °C with Et₂O separated two yellow fractions. Solvent was removed from each, and both products were recrystallized from Et₂O (2 mL) by cooling to –78 °C. Thus, two microcrystalline yellow samples were obtained and identified in the usual manner, as compounds **10a** (0.050 g, 45% yield) and **4a** (0.047 g, 42% yield), respectively.

X-ray Crystal Structure Determinations. The crystal data and other experimental details for compounds **9a, 11b,** and **12b** are summarized in Table VI. Crystals of **9a** were grown by the slow diffusion of Et₂O into a THF solution of the complex at 0 °C, those of **11b** from *n*-hexane (–20 °C), and those of **12b** by the slow diffusion of petroleum ether into a CH₂Cl₂ solution of the complex at ambient temperatures. For compound **9a** the asymmetric unit contains half a molecule of THF, which is disordered about the inversion center (0, 0.5, 0.5). The presence of THF was confirmed by recording a ¹H NMR spectrum of the same batch of crystals.

All data were corrected for Lorentz, polarization, and X-ray absorption effects, the latter by an empirical method based on azimuthal scan data.[19] The structures were solved by Patterson and difference Fourier

methods, by which all non-hydrogen atoms were located and refined with anisotropic thermal parameters. The carborane cage hydrogen atoms of **11b** were directly located and refined without positional constraints but with fixed isotropic thermal parameters (U_{iso} = 0.08 Å²). All other hydrogen atoms were included at calculated positions (C–H, 0.96; B–H, 1.1 Å²⁰) with fixed isotropic thermal parameters ($1.2U_{equiv}$ of the parent carbon or boron atom).

Calculations were performed on a Digital micro-vax II computer with the SHELXTL PLUS suite of programs.[19] Atomic scattering factors with corrections for anomalous dispersion are inlaid in the programs.

Supplementary Material Available: Microanalytical data for all new compounds and complete crystallographic structure determination descriptions for **9a, 11b,** and **12b** and tables of atomic coordinates, complete lists of bond lengths and angles, and anisotropic displacement coefficients for compounds **9a, 11b,** and **12b** (32 pages); listings of observed and calculated structure factors (67 pages). Ordering information is given on any current masthead page.

(19) Sheldrick, G. M. SHELXTL PLUS programs for use with the Siemens R3m/V X-ray system.

(20) Sherwood, P. BHGEN—a program for the calculation of idealized H-atom positions for a nido-icosahedral carborane fragment, Ph.D. Thesis, University of Bristol, 1986.

Bond-Stretch Isomerism in the Complexes *cis-mer*-MoOCl₂(PR₃)₃: A Reinvestigation

Keum Yoon,† **Gerard Parkin,***,† **and Arnold L. Rheingold**‡

Contribution from the Departments of Chemistry, Columbia University, New York, New York 10027, and University of Delaware, Newark, Delaware 19716. Received September 6, 1991

Abstract: The molecular structures of a series of complexes *cis-mer*-MoOCl₂(PR₃)₃ (PR₃ = PMe₃, PMe₂Ph) have been investigated by X-ray diffraction methods. The data indicate a large range of apparent Mo=O bond lengths. The apparent lengthening of the Mo=O bond in these complexes is rationalized in terms of compositional disorder with the isostructural trichloride derivative *mer*-MoCl₃(PR₃)₃. These results suggest that, contrary to the original suggestion (Chatt, J.; Manojlovic-Muir, L.; Muir, K. W. *Chem. Commun.* **1971,** 655–656), there is no evidence for bond-stretch or distortional isomerism for the *cis-mer*-MoOCl₂(PR₃)₃ system.

Introduction

More than 20 years ago, Butcher and Chatt reported a series of octahedral molybdenum oxo complexes with a meridonal arrangement of phosphine ligands, *mer*-MoOX₂(PR₃)₃ (X = Cl, Br, I, NCO, NCS; PR₃ = PMe₂Ph, PEt₂Ph, PPrⁿ₂Ph, PBuⁿ₂Ph, PMePh₂, PEtPh₂, PPrⁿPh₂, MeC[CH₂PPh₂]₃).[1] The complexes *mer*-MoOX₂(PR₃)₃ were either blue or green, depending upon the nature of both X and PR₃. However, one of these complexes, *mer*-MoOCl₂(PMe₂Ph)₃, could be isolated in *both* blue and green isomeric forms. The blue and green isomers had very similar melting points (blue, 155–157 °C; green 153–156 °C) but different ν(Mo=O) stretching frequencies (blue, 954 cm⁻¹; green, 943 cm⁻¹) and were originally proposed to be *geometric* isomers, namely *cis-mer*-MoOCl₂(PMe₂Ph)₃ and *trans-mer*-MoOCl₂(PMe₂Ph)₃, differing only in whether the two chloride ligands were cis or trans. Single-crystal X-ray diffraction established a cis configuration

of chloride ligands for the blue isomer, i.e., *cis-mer*-MoOCl₂-(PMe₂Ph)₃, from which it was concluded that the green isomer (and, hence, *all* the green complexes) possessed a trans configuration, as illustrated in Figure 1. However, following the original report,[1] Chatt, Manojlovic-Muir, and Muir determined the molecular structure of the green complex *mer*-MoOCl₂(PEt₂Ph)₃ and found, to their surprise, that the chloride ligands were cis and *not* trans.[2] Although the alkyl substituents on the phosphine ligands adopted different orientations in blue *cis-mer*-MoOCl₂(PMe₂Ph)₃ and green *cis-mer*-MoOCl₂(PEt₂Ph)₃, the coordination environments around the molybdenum centers were similar for both molecules, with the exception that the Mo=O bond length in green *cis-mer*-MoOCl₂(PEt₂Ph)₃ (1.803 (11) Å) was *significantly* longer than that observed in blue *cis-mer*-MoOCl₂(PMe₂Ph)₃ (1.676 (7)

(1) Butcher, A. V.; Chatt, J. *J. Chem. Soc. A* **1970,** 2652–2656.
(2) (a) Chatt, J.; Manojlovic-Muir, L.; Muir, K. W. *Chem. Comm.* **1971,** 655–656. (b) Manojlovic-Muir, L. *J. Chem. Soc. A* **1971,** 2796–2800. (c) Manojlovic-Muir, L.; Muir, K. W. *J. Chem. Soc., Dalton Trans.* **1972,** 686–690.

† Columbia University.
‡ University of Delaware.